Experimental study of a venturi ejector for passive recirculation of hydrogen in PEM fuel cell systems

Pedro Miguel Henriques Pires da Silva Rodrigues
pedro.silva.rodrigues@tecnico.ulisboa.pt

Instituto Superior Técnico, Universidade de Lisboa, Portugal

July 2022

Abstract

This study explores an opportunity to increase a PEM fuel cell system efficiency by replacing an energy-demanding pump with a passive device, a venturi ejector, to perform hydrogen recirculation in the fuel cell's anode. An experimental approach to this subject was taken where multiple factors that characterize the working environment of a PEMFC were studied. Namely, I-V curves were obtained, hydrogen and air flow rates were measured, the pressure drop in the anode was recorded, as well as the inlet temperature and relative humidity. These variables were obtained for a system set-up in open anode, encompassing a diaphragm pump and a venturi ejector. The results of this study partially validate the utilization of the venturi ejector. The study showed that the systems provide similar and stable I-V curves, hydrogen and air flow consumption profiles, and anode and cathode pressure drops. Nevertheless, the recirculation flow rate imposed by the venturi ejector seems insufficient to keep a recommended anode relative humidity above 40%, at stack temperature, 65°C. Finally, the utilization of the venturi ejector for hydrogen recirculation results in a 60% energy saving compared to the utilization of the pump.

Keywords: PEM fuel cell, Active recirculation, Passive recirculation, Venturi ejector

1. Introduction

The World Meteorological Organisation (WMO) reported that 2020 was one of the three warmest years on record [22], Figure 1. The Paris Agreement defines in Article 2 - 1 (a) that the global average temperature rise should be held to 2 ºC and preferably to 1.5ºC above pre-industrial levels [2]. The European Union (EU) and its Member States, acting jointly, are committed to a binding target of a net domestic reduction of at least 55% in greenhouse gas emissions by 2030 compared to 1990 [3]. Hydrogen (H_2), as a key energy transition pillar, is gathering a strong momentum with over 30 countries having released hydrogen road maps, more than 200 hydrogen projects announced by the industry, over USD 70 billion in public funding and an additional investment of USD 300 billion from the private sector. Moreover, Hydrogen Council now represents a 6.6 trillion market capitalization with more than 6.5 million employees [9, 1]. Portugal and The Netherlands, where the present work was conducted, aim to have installed 4 GW and 2 GW of electrolyser capacity by 2030, respectively, for green hydrogen production [16, 18, 17].

In the effort to contribute to these goals this work tackles a very small part of the solution. Hydrogen recirculation in PEMFCs is a key factor for the efficiency of the energy generation process [13, 6, 15]. Current hydrogen recirculation processes are in its majority addressed via active recirculation, meaning, with the usage of a pump, increasing energy consumption and consequently decreasing efficiency [12, 8]. Passive recirculation using a venturi ejector is a potential alternative [21, 14]. The fact that its operation is strictly mechanical and so, no electricity required for operation, there is the potential to furthermore increase the efficiency of energy generation in PEMFCs [11]. A venturi ejector converts potential energy from the high-pressure hydrogen tank into kinetic energy and the increased flow velocity through a tapered nozzle forms a vacuum area at the exit of the nozzle dragging the recirculated flow [4]. The entrainment flow is then a mixture of dry hydrogen (H_2) and high relative humidity (RH%) hydrogen that has the required properties for anode inlet in PEMFCs [19].

1.1. State of the art

The literature has seen an increasing number of studies in recent years concerning the use of a venturi ejector in PEMFC systems. However, the first link between a venturi ejector and PEMFC was es-

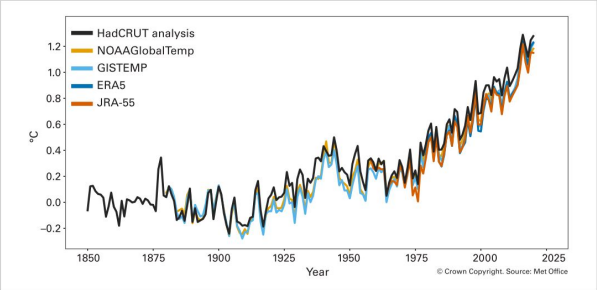

Figure 1: Global annual mean temperature difference from pre-industrial conditions (1850–1900) for five global temperature data sets.

tablished in 2003 when McCurdy *et al.* [10] applied one to oxygen recycling in space power applications [6]. Recently, most studies address the influence of ejector geometry in different factors or simply study the performance of an ejector in different operating conditions. However, there are few studies that compare the performance of an ejector against an active pump, in particular, an experimental comparison of both mechanisms could not be found. Huang *et al.* [7] created a model of a recirculation system where they compared the total efficiency of the system with active and passive recirculation. The latter registered a higher efficiency, as expected. Moreover, they proved that the recirculation mechanisms are influenced by the pressure at hydrogen outlet concluding that higher pressure means higher recovery rate. The efficiency of the system could also be increased by increasing the temperature of the hydrogen supply in constant flow. Toghyani *et al.* [20] developed a thermodynamic model for an ejector and an electrochemical pump. They verified that increasing the working temperature increases the performance of both the ejector and the electrochemical pump, that the recirculation ratio and hydrogen stoichiometric of the ejector increase at higher operating point and that the increase of hydrogen RH% leads to an increase of the secondary mass flow rate of the ejector leading to higher recirculation ratio.

2. Experiment

2.1. Setup

The experimental set-up consists of a test station designated by KTS, depicted in Figure 2. It encompasses all the equipment used to measure and control temperature, pressure, flow and relative humidity of hydrogen, H_2, and air. The temperature and flow of cooling water are also measured and controlled. KTS is used for performance measurement of stacks from 3 to 44 cells under different operating conditions. In order to conduct this work it was necessary to perform changes to the configuration of the test station. Two hydrogen recirculation loops were assembled. The first loop consists on the active recirculation system and is composed by a drain vessel and a diaphragm hydrogen pump. A pressure regulator and a relief valve were also installed. The relief valve protects the system from over-pressures and the pressure regulator on the active recirculation system allows setting the pressure to the working pressure of the PEMFC. The second loop consists on the passive recirculation system and is composed by a drain vessel and the venturi ejector.

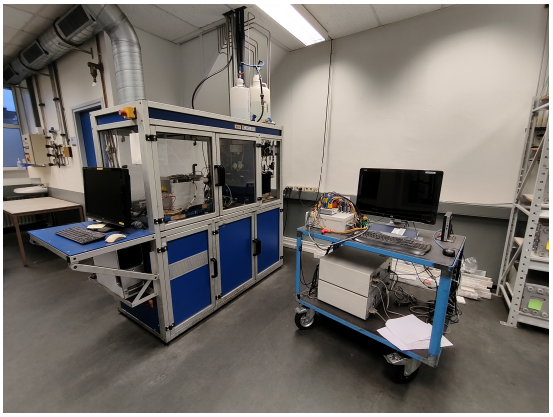

Figure 2: Test station: KTS.

2.2. Nedstack®'s 5.5 kW PEMFC

The PEMFC allocated to this experiment consists of a Gen 2.51 with serial number S2397, Figure 3. It is composed by 44 cells with an active area of 200 cm^2 and a maximum power output of approximately 5.5 kW. At maximum power the PEMFC will consume 88 Nl/min of hydrogen, H_2, and 335 Nl/min of air. The optimal working temperature is 65ºC. This PEMFC was built for research purposes only.

Figure 3: Nedstack®'s 5.5 kW PEMFC.

2.3. Diaphragm hydrogen pump

Current operating systems use claw pumps to maintain a constant flow of hydrogen recirculating. For the 5.5 kW PEMFC in use, a 24 V KNF diaphragm pump with the part number N838KNDC fills the requirement of constantly flowing humidified hydrogen. In the case of this study, substituting an energy demanding device like a pump by a passive component like a venturi ejector completely eliminates the parcel of the system's efficiency decrease due to the use of a pump.

2.4. HyLoop®

HyLoop® is a product of Ad-Venta INNOVATIVE. HyLoop® is a plug and play solution that integrates a control system that ensures the correct functioning of the venturi ejector. It is composed by a proportional solenoid valve, a pressure relief valve, two pressure and one temperature sensors as well as a control unit, Figure 4. HyLoop® guarantees a minimum recirculation percentage of 50% and a maximum of 225% which means that at least half and a maximum of twice the input flow is recirculated.

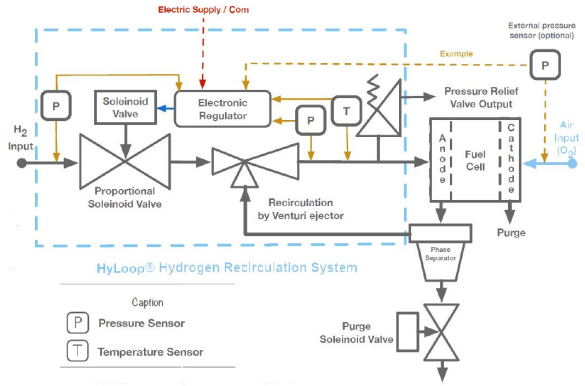

Figure 4: HyLoop®'s P&ID.

2.5. Acquisition System

The acquisition system is composed by pressure, temperature and humidity sensors on the anode inlet and outlet of the PEMFC in order to measure the differential between both terminals. Mass flow meters/controllers are placed upstream the entire system to measure the exact quantity of hydrogen, H_2, and air being consumed. HyLoop® encompasses a control unit that allows the user to set the desired outlet pressure of hydrogen. The pressure setting is done recurring to a PEAK connection and using the software provided by the manufacturer, HyLoop2020CanMonitoring®.

2.6. Procedure

Two groups of experiments were performed, ahead designated by G1 and G2. G1 corresponds to 3 sets of I-V curves (basic performance) for the three

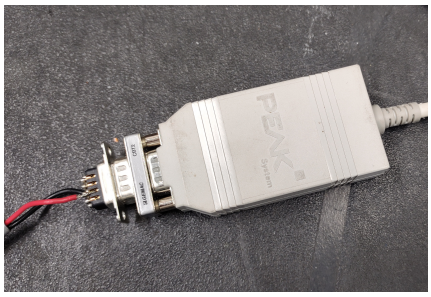

Figure 5: CAN-BUS interface: PEAK with 120 Ω DB9 connector.

system set-ups and G2 to one start-up/shutdown sequence for all set-ups and three ramp-up/ramp-down sequences also for the three set-ups. First, the PEMFC is placed in the KTS and all the piping and electrical cables are connected. The temperature of the PEMFC is increased to the operation set-point of 65ºC by passing hot water from an external source trough the cooling conduits of the PEMFC. Once it reaches the required temperature both the anode and cathode are flushed with nitrogen, N_2, in order to clear the channels of any other gases and water droplets. Afterwards, hydrogen floods the anode side and air the cathode side bringing the stack to OCV. At this point a load controlled by LabView is used to draw a user defined current from the PEMFC. At this point the heat source heating the cooling water has already been turned off and the flow adjusts automatically to keep a constant inlet temperature of 65ºC. For the I-C curve tests, the current is firstly increased to 40 A and afterwards from 40 A to 160 A in steps of 20 A. For the stress tests and start-up/sutdown procedure, the current is instantaneously increased from 0-40 A and decreased from 40-0 A, after voltage stabilization. For the stress tests and ramp-up/ramp-down procedure, the current is instantaneously increased from 40-120 A and decreased from 120-40 A, after voltage stabilization. For active recirculation, the subsystem presented in Figure 6 is installed in the KTS and the same procedure is performed.

(a) Low pressure regulator and pressure relief valve

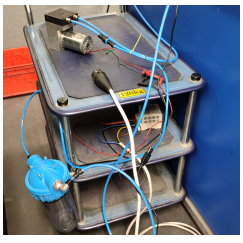

(b) Drain vessel and hydrogen recirculation pump

Figure 6: Active recirculation system assembly.

For passive recirculation, the subsystem presented in Figure 7 is installed in the KTS and the same procedure is performed.

(a) 500Nl/min flow meter

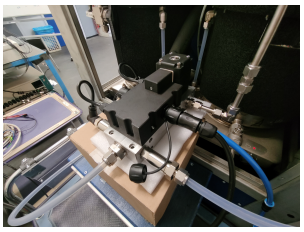

(b) HyLoop®

Figure 7: Passive recirculation system assembly.

3. Models

3.1. Hydrogen Inlet Flow

The inlet flow of a stack accounts for the amount of hydrogen needed for the correct operation of a stack at a given current. Equation 1 describes the behaviour of hydrogen inlet flow as the current produced by the stack increases. Equation 2 accounts for the minimum amount of hydrogen that should be supplied to the stack at any point of operation.

$$\dot{V}_{H_2inlet} = 1.25 \times 10^{-3} \times n \times I\,(Nl/min),\ I > 40A. \quad (1)$$

$$\dot{V}_{H_2mininlet} \geq 0.6 \times n\,(Nl/min),\ I \leq 40A. \quad (2)$$

3.2. Hydrogen Recirculation

The recirculation of hydrogen is performed in excess in the entire span of operation. Equation 3 describes its behaviour. The factor 2.5 accounts for the stoichiometry of recirculated hydrogen, n, represents the amount of cells in the stack and I_{max} stands for the maximum recommended current produced by stack, 230 A.

$$\dot{V}_{H_2recycled} = 2.5 \times 10^{-3} \times n \times I_{max}.5cm(Nl/min). \quad (3)$$

3.3. Hydrogen Consumption

The amount of hydrogen consumed in the stack is given by Faraday's law which can be translated for this stack in Equation 4.

$$\dot{V}_{H_2consumed} = 6.965 \times 10^{-3} \times n \times I.05cm(Nl/min). \quad (4)$$

3.4. Anode Pressure Drop

The stack pressure drop increases linearly with the inlet gas flow. Equation 5 gives the typical anode pressure drop for the stack under normal operating conditions. Equation 6 gives the minimum pressure drop in the anode.

$$\Delta P_{H_2} = 0.2 \times I + 1.4\,(mbar),\ I > 40A. \quad (5)$$

$$\Delta P_{H_2} = 15\,(mbar)\,, I \leq 40A. \quad (6)$$

3.5. Air Inlet Flow

The inlet flow of air in a stack accounts for the amount of air needed for the correct operation of a stack at a given current. Equation 7 describes the behaviour of the air inlet flow as the current produced by the stack increases. Equation 8 accounts for the minimum amount of air that should be supplied to the stack at any point of operation. It depends only on the number of cells of the stack, n, which in this case equals 44.

$$\dot{V}_{airinlet} = 1.25 \times 10^{-3} \times n \times I\,(Nl/min)\,, I > 40A. \quad (7)$$

$$\dot{V}_{airmininlet} \geq 1 \times n\,(Nl/min)\,, I \leq 40A. \quad (8)$$

3.6. Air Pressure Drop

The stack pressure drop in the cathode increases linearly with the inlet flow. Equation 9 gives the typical cathode pressure drop for the stack under normal operating conditions. Equation 10 gives the minimum pressure drop in the cathode.

$$\Delta P_{Air} = 0.2 \times I + 1.4\,(mbar),\ I > 40A. \quad (9)$$

$$\Delta P_{Air} = 15\,(mbar)\,, I \leq 40A. \quad (10)$$

3.7. Venturi Ejector

The equations that rule the behaviour of hydrogen in the ejector present in the HyLoop® are not known due to the fact that these are proprietary technology of Ad-venta®. Nevertheless, a relation between the recirculation ratio and the injected flow was provided together with the product's datasheet and Equation 11 represents an extrapolated equation obtained from this graph where phi, Φ, is the recirculation ratio and $\dot{V}$ represents the ejector's inlet flow.

$$\Phi = -0.012\dot{V}_{H_2inlet} + \dot{V}_{H_2inlet} + 207\ \ (\%). \quad (11)$$

3.8. PEMFC I-V Curve

The I-V curve, or polarization curve, is the most common method of characterizing a fuel cell. The I-V curve taken as reference is the one obtained from a DQC (Detailed Quality Control) test of the stack, Figure 8. DQC is the standard test used

for product approval. It is performed with open anode and consists of drawing a fixed current from the fuel cell and measuring the output voltage. In this case the current is varied from 0A to 298A. For this stack, in normal operation, the current drawn should stay within 40A to 230A, in order to extend its life time.

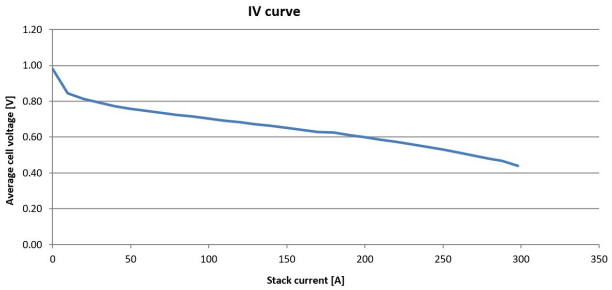

Figure 8: Stack's I-V curve obtained from the DQC test @1.25 stoichiometry in the anode and @2.0 stoichiometry in the cathode. PEMFC @65°C.

4. Results

4.1. I-V Curve

The open anode, pump and ejector's I-V curves obtained with the KTS were compared to the BOL I-V curve and to a 5-HP kWe and 7-XXL kWe stack I-V curves, both commercial stacks. A thorough analysis of the results shows an average difference between voltage values of the two I-V curves of 2%. This value brings more relevance to the results further obtained given the fact that these won't be significantly affected by decaying effects on the stack. Figure 9 depicts an average of the I-V curves of the pump and the ejector compared to the 5-HP kWe and 7-XXL kWe stack I-V curves. A brief analysis of the curves seems to indicate a satisfactory operation of the stack with both set-ups. The average relative errors between the pump and ejector average curves when compared to the DQC curve are 2.1% and 1.1%, respectively. The absolute average difference voltage between both set-ups is 0.3 V.

4.2. Hydrogen Inlet

The consumption of Hydrogen is expected to have significantly different values when recirculation is in place when compared to the model supplied in the stack manual [5]. As with the test station used, the stack manual considers the use of the fuel cell in open-anode, although it is not the case when a stack integrates a system. The stack manual considers a stoichiometry of 1.25 for the hydrogen supply. In open-anode operation this amount of hydrogen is not consumed and as such, it is released to the atmosphere. Implementing a recirculation system means that only the flow of hydrogen being consumed is being supplied to the stack resulting in a

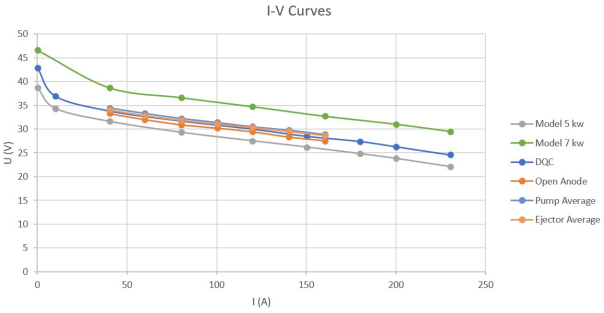

Figure 9: Experimental averaged I-V curves collected for all three set-ups: OA @1.25 stoichiometry, Ejector and Pump @1.0 stoichiometry compared to 5kW and 7kW model I-V curves. PEMFC @65°C.

stoichiometry of 1.0. Figure 10 depicts an average of the hydrogen consumption of the pump and the ejector. Considering the area of interest between 80 A and 160 A, the average relative difference between the Model @1.0 and the pump and ejector set-up is 2.4% and 2.8%, respectively. Also, the average relative difference between the DQC hydrogen consumption and the pump and ejector set-up's hydrogen consumption is -20.2% and -19.9% respectively, meaning this percentage is being saved just by adding a recirculation system. The hydrogen consumption absolute average difference between the pump and ejector set-up is 0.26 Nl/min. This is a considerably low value and as such does not represent a relevant meaning. In fact it is 100x smaller than the flows being measured at low currents and 250x smaller than the flows at high currents. Overall, these results show a positive tendency towards the possibility of replacing the pump for the ejector.

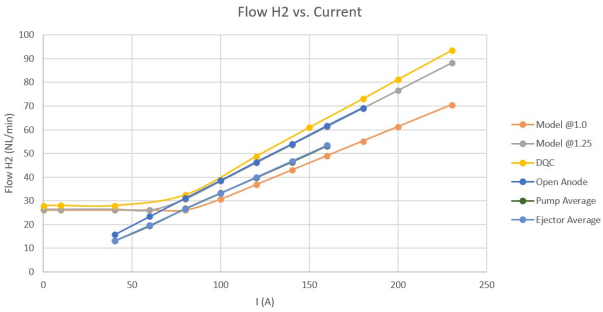

Figure 10: Experimental results for average hydrogen consumption collected for all three set-ups: OA, Ejector and Pump compared to DQC and the extrapolated model as described in Section 3 at 1.0 and 1.25 stoichiometry. PEMFC @65°C.

4.3. Air Inlet

Air circulation in the cathode is independent from having hydrogen recirculation in place or not.

Therefore it is expected that the air flow in the cathode varies in the same manner for all three set-ups. In order to facilitate processing the data, an average of the $\dot{V}_{Airinlet}$ curves of the pump and the ejector was obtained and is depicted in Figure 11. As expected it shows an almost coincidence of points apart for the one at current, I, equal to 120 A, for the reasons explained above. A thorough analysis shows that the pump set-up presents a 0.6% and a 5.5% average deviation between the DQC and Model @2.0, respectively and the ejector set-up shows a 0.1% and 6% average deviation between the DQC and Model @2.0, respectively.

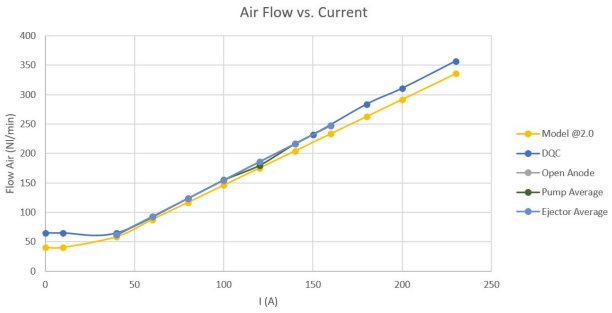

Figure 11: Experimental average results for air consumption collected for all three set-ups: OA, Ejector and Pump compared to DQC and the extrapolated model as described in Section 3 at 2.0 stoichiometry. PEMFC @65°C.

4.4. Relative Humidity

Hydrogen recirculation plays a key role in humidifying the cells membrane. According to the stack manual [5], hydrogen inlet humidity should be kept at least at 40% at stack temperature, 65°C. The pump originates a RH% similar to the open-anode and around 100%, according to the graph, whereas the RH% profile of the ejector tests is situated between 40-80%. In order to easily analyse these values, the average of the RH% and temperature curves of the two set-ups was considered and presented in Figure 12 and Figure 13.

Regarding Figure 13, it's possible to conclude that the temperature of the open-anode set-up is relatively stable and just below 55°C and that the temperature profiles of both the pump and the ejector set-ups tend to 35°C approximately. This means that exists approximately a 20°C difference between no-recirculation and recirculation operation. Finally, the fact that for the same temperature, the ejector shows less RH% than the pump RH% profile, might indicate that the ejector is not able to cope with the RH% demand of 40% at stack temperature, 65°C, at least in the range of operation of 40-160 A. In fact, according to the calculations internally performed, at 65°C and 40% humidity, the

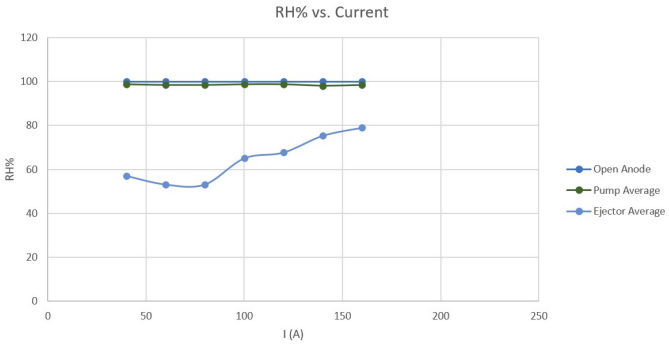

Figure 12: Experimental results for average relative humidity collected for all three set-ups: OA @1.25 stoichiometry, Ejector and Pump @1.0 stoichiometry. PEMFC @65°C.

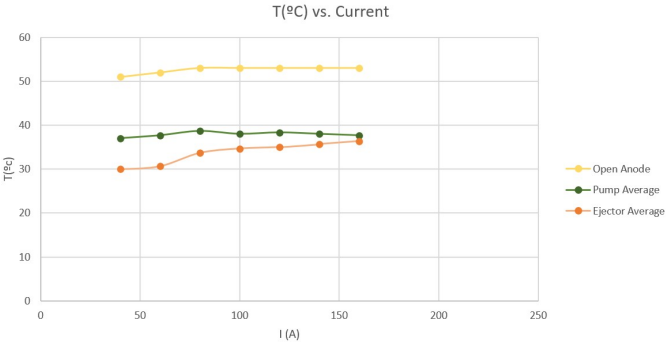

Figure 13: Experimental results for average inlet temperature collected for all three set-ups: OA @1.25 stoichiomtry, Ejector and Pump @1.0 stoichiomtry. PEMFC @65°C.

dew point temperature, $T_{dewpoint}$, is 43.7°C. So, for the same dew point, at 35°C, the relative humidity should be 152%. This means that for the ejector set-up there's possibly a too low RH% at stack inlet since the results obtained show an RH% between 50% and 80% and not of 100% or above as for the pump.

4.5. Anode and Cathode Pressure Drops

The pressure drop across the anode is a good indicator of the flow trough the channels. Higher the flow implies higher pressure drop. An analysis of the results was performed considering the average values of the anode and cathode pressure drops of all tests for both set-ups and is depicted in Figure 14. As expected, the cathode pressure drop stays unaltered in both situations whereas for the anode side, a significant difference is observed. The fact that the pressure drop originated by the ejector set-up under 100 A is lower than the one from the pump set-up indicates that the flow recirculated is also smaller than the flow recirculated by the pump. The opposite occurs above 100 A. An analysis to the

recirculated flow is elaborated in Section 4.6. Figure 14 also indicates a maximum difference between both set-ups of approximately 10 mbar. This difference is 10% of the maximum design back-pressure of the ejector, 100 mbar.

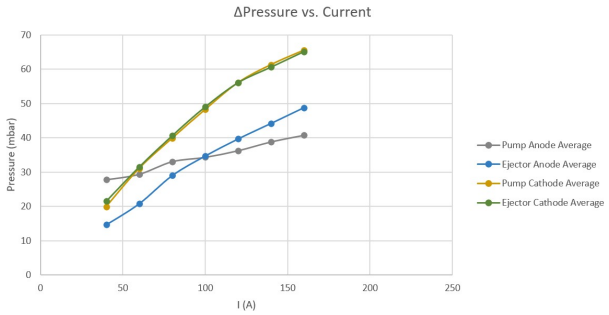

Figure 14: Experimental average results for the anode, @1.0 stoichiometry and cathode @2.0 stoichiometry, pressure drops collected for the ejector and Pump set-ups. PEMFC @65°C.

4.6. Recirculated Flow

Measuring the actual flow in the recirculation loop allows to validate the characteristics of the ejector as described in Section 3.7. Nevertheless, this proved not no be an easy task. Due to the fact that the stack outlet gas from the anode presents very high humidity, the flow meters available wouldn't get comprehensive readings on the anode outlet flow rate. Therefore a comparative approach was undertaken knowing that there is a relation between the pressure drop across the anode and the stoichiometry. In order to have both the ejector test and the

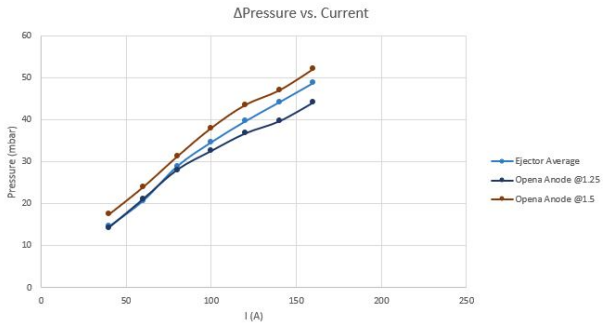

Figure 15: Pressure drop interpolation in the anode @1.25 stoichiometry. PEMFC @65°C.

open anode at the same conditions, meaning, same dew point, the correspondent open anode temperature and humidity was calculated. For a temperature of 35ºC and 80% humidity of the inlet gas in the ejector set-up, the correspondent open anode temperature and relative humidity are 65ºC and 30%, respectively. Knowing these values, they were inserted in the KTS and two open-anode I-V curve tests were performed for 1.25 and 1.5 stoichiometry. The results for the pressure drop measured are presented in Figure 15. As for the previous sections, the point at 100 A marks a transition of the behaviour of the curve. A further analysis indicates that under 100 A the stoichiometry produced by the ejector is approximately 1.25 and above 1.4. This allows to obtain the actual flow being recirculated as depicted in Figure 16. The figure shows that the ejector seems to be performing under the minimum theoretical curve. In order to better understand

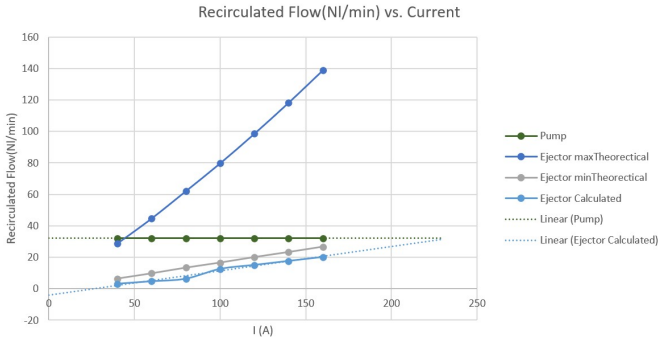

Figure 16: Recirculation ratio for the Pump and Ejector set-ups. The ejector recirculated flow is obtained from the interpolated stoichiometry. Maximum and minimum theoretical recirculation flows of the ejector are presented. Anode stoichiometry @1.0 and PEMFC @65°C.

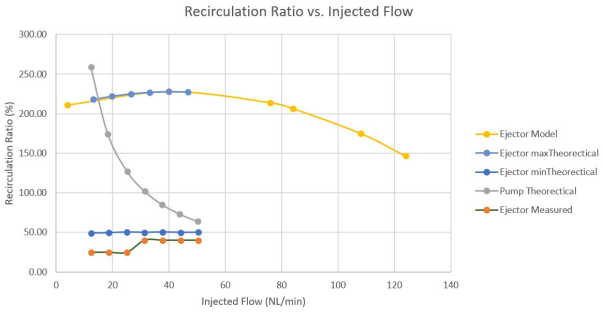

Figure 17: Recirculation ratio for the Pump and Ejector set-ups. The ejector recirculated flow is obtained from the interpolated stoichiometry. Maximum and minimum theoretical recirculation flows of the ejector are presented. Anode stoichiometry @1.0 and PEMFC @65°C.

the results obtained, the same results obtained were organized and presented in a different form in Figure 17, in order to match the performance graph shown in the ejector's data sheet. The figure clearly shows that the extracted results are approximately situated in the first half of the performance curve. In the case of the pump set-up, the curve evolves as expected from a stoichiometry of approximately 3.5 to 1.5. In the case of the ejector and as with

Figure 16, it's visible that the ejector is performing under the minimum theoretical curve. A main concern is that there might be too much water entering the ejector making it under perform. A reason for this suspicion is that the drain vessel did not included a filter which considerably improves the retention of water droplets. In fact upon disassemble of the ejector, a considerable amount of water was removed from the ejector's secondary inlet. Yet, another conclusion form this graphic is that the recirculation ratio might increase with current, I, as such, to perform a study on the full performance curve of the ejector might bring better understanding on it's behaviour under these conditions.

4.7. Start-up/Shutdown

The objective of studying the behaviour of the ejector during start-up/shutdown is to verify if it is capable of dealing with a sudden no-flow to minimum flow situation and the opposite. The results showed that the ejector does not affect the start-up of the stack/system since the reaction of the voltage in every cell is apparently almost instantaneous. The same can be observed during shut-down.

4.8. Ramp-up/Ramp-down

In a PEM fuel cell system application, the energy demand is expected to be instantaneous. In that regard, the components around the stack should allow an instantaneous energy production. The results showed that the ejector does not affect the ramp-up of the stack/system since the reaction of the voltage in every cell is apparently almost instantaneous. The same can be observed during ramp-down.

4.9. Efficiency of pump-driven and ejector-driven recirculation

Depending on the pump at use and the size of the system where it is installed, the weight of its power consumption on the overall system efficiency varies. For this case, the pump in use was a KNF N838KNDC that consumes 45.6 W at max power.
In the case of the ejector, although the ejector itself is a mechanical device and as such does not consume energy, the peripheral system mounted around it in order to control the pressure downstream does. The HyLoop v4® at max flow has a power consumption of 18 W.
This represents a decrease of 60.5% of the energy requirement for hydrogen recirculation in the anode. Whether or not this value has relevance when compared to the overall system energy losses requires further analysis.

5. Conclusions

The main goal of this work was to provide an insight on the use of ejectors for hydrogen recirculation in PEMFC systems. The important findings of this thesis are summarized and listed below:

1. Using an ejector as an alternative to pump-driven hydrogen recirculation proved to partially meet the goals stated in Section 1.6. Although the ejector proved to allow stable recirculation as well as instantaneous response to ramp-up/ramp-down procedures, it seems to fail to provide satisfactory anode humidification.

2. The hydrogen recirculation flow measured experimentally was not consistent with the stated in the product data-sheet. Although it was not expected to meet the maximum recirculation profile due to the fact that hydrogen with high RH% was being used, it was expected to perform above the minimum theoretical recirculation curve. A reason for this could be the presence of water droplets in the ejector's secondary inlet.

3. The expected stoichiometry of approximately 1.0 for the main hydrogen supply was obtained when implementing recirculation allowing savings of 25% of the hydrogen used. The air stoichiometry stayed unaltered at 2.0.

4. The average deviation of the I-V curves of the ejector and the pump have an absolute average difference of 0.3V. This value is less than 1% of the lowest operating voltage registered for the OA set-up, 27.5 V.

5. The anode pressure drop originated by the pump under 100 A is higher than the one originated by the ejector and the opposite occurs above 100 A. They differ a maximum of 15 mbar which occurs at 40 A.

6. The ejector seems not to work properly below 100 A since it presents a considerably low recirculation ratio. Nevertheless it shows a tendency of increasing recirculation ration with the increase of current. I.

7. The ejector showed no signs of being affect by starting-up and shutting-down procedures as well as by 80 A interval ramp-up/ramp-down requests, demonstrating instantaneous response.

8. Replacing the pump for the venturi ejector would result in a reduction of 60% of energy savings for hydrogen recirculation in the anode.

Acknowledgements

The author would like to thank Nedstack Fuel Cell Technology B.V. for the support throughout the duration of this project.

References

[1] Global Hydrogen Review 2021. *Global Hydrogen Review 2021*, 2021.

[2] J. Delbeke, A. Runge-Metzger, Y. Slingenberg, and J. Werksman. The paris agreement. *Towards a Climate-Neutral Europe: Curbing the Trend*, pages 24–45, 2019.

[3] European Commission. Update of the NDC of the European Union and its Member States. (December):1–19, 2020.

[4] M. L. Ferrari, M. Pascenti, and A. F. Massardo. Validated ejector model for hybrid system applications. *Energy*, 162:1106–1114, 2018.

[5] N. fuel cell technology B.V. . Installation and Operation Manual Nedstack PEM Fuel Cell Stack. 2010.

[6] Z. Hailun, W. Sun, H. Xue, W. Sun, L. Wang, and L. Jia. Performance analysis and prediction of ejector based hydrogen recycle system under variable proton exchange membrane fuel cell working conditions. *Applied Thermal Engineering*, 197(July):117302, 2021.

[7] P. H. Huang, J. K. Kuo, W. Z. Jiang, and C. B. Wu. Simulation analysis of hydrogen recirculation rates of fuel cells and the efficiency of combined heat and power. *International Journal of Hydrogen Energy*, 46(31):16823–16835, 2021.

[8] J. J. Hwang. Passive hydrogen recovery schemes using a vacuum ejector in a proton exchange membrane fuel cell system. *Journal of Power Sources*, 247:256–263, 2014.

[9] Hydrogen Council. Hydrogen Insights. (February):58, 2021.

[10] A. V. K. B. K. McCurdy. Development of PEMFC systems for space power applications. pages 1–7, 2003.

[11] F. Li, J. Du, L. Zhang, J. Li, G. Li, G. Zhu, M. Ouyang, J. Chai, and H. Li. Experimental determination of the water vapor effect on subsonic ejector for proton exchange membrane fuel cell (PEMFC). *International Journal of Hydrogen Energy*, 42(50):29966–29970, 2017.

[12] Y. Liu, Z. Tu, and S. H. Chan. Applications of ejectors in proton exchange membrane fuel cells: A review. *Fuel Processing Technology*, 214(October 2020):106683, 2021.

[13] Y. Liu, B. Xiao, J. Zhao, L. Fan, X. Luo, Z. Tu, and S. Hwa Chan. Performance degradation of a proton exchange membrane fuel cell with dual ejector-based recirculation. *Energy Conversion and Management: X*, 12:100114, 2021.

[14] K. Nikiforow, P. Koski, and J. Ihonen. Discrete ejector control solution design, characterization, and verification in a 5 kW PEMFC system. *International Journal of Hydrogen Energy*, 42(26):16760–16772, 2017.

[15] K. Nikiforow, J. Pennanen, J. Ihonen, S. Uski, and P. Koski. Power ramp rate capabilities of a 5kW proton exchange membrane fuel cell system with discrete ejector control. *Journal of Power Sources*, 381(September 2017):30–37, 2018.

[16] NL Netherlands. Excelling in Hydrogen: Dutch technology for a climate-neutral world. 2021.

[17] República Portuguesa. Estratégia Nacional-H2. 2020.

[18] A. e. A. C. República Portuguesa and Direção Geral de Energia e Geologia. *Roteiro e plano de ação para o hidrogénio em portugal*. 2019.

[19] B. M. Tashtoush, M. A. Al-Nimr, and M. A. Khasawneh. A comprehensive review of ejector design, performance, and applications. *Applied Energy*, 240(January):138–172, 2019.

[20] S. Toghyani, E. Afshari, and E. Baniasadi. A parametric comparison of three fuel recirculation system in the closed loop fuel supply system of PEM fuel cell. *International Journal of Hydrogen Energy*, 44(14):7518–7530, 2019.

[21] X. Wang, S. Xu, and C. Xing. Numerical and experimental investigation on an ejector designed for an 80kW polymer electrolyte membrane fuel cell stack. *Journal of Power Sources*, 415(October 2018):25–32, 2019.

[22] WMO. *State of the Global Climate 2020*. Number 1264:56. 2021.